Time-dependent multiconfiguration theory for electronic dynamics of molecules in intense laser fields: A description in terms of numerical orbital functions

Tsuyoshi Kato and Hirohiko Kono

Citation: J. Chem. Phys. **128**, 184102 (2008); doi: 10.1063/1.2912066
View online: http://dx.doi.org/10.1063/1.2912066
View Table of Contents: http://jcp.aip.org/resource/1/JCPSA6/v128/i18
Published by the American Institute of Physics.

Time-dependent multiconfiguration theory for electronic dynamics of molecules in intense laser fields: A description in terms of numerical orbital functions

Tsuyoshi Kato[1,a)] and Hirohiko Kono[2,b)]
[1]*Department of Chemistry, School of Science, The University of Tokyo, 7-3-1 Hongo, Bunkyo-ku, Tokyo 113-0033, Japan*
[2]*Department of Chemistry, Graduate School of Science, Tohoku University, Sendai 980-8578, Japan*

(Received 3 March 2008; accepted 27 March 2008; published online 9 May 2008)

The equations of motion (EOMs) for spin orbitals in the coordinate representation are derived within the framework of the time-dependent multiconfiguration theory developed for electronic dynamics of molecules in intense laser fields. We then tailor the EOMs for diatomic (or linear) molecules to apply the theory to the electronic dynamics of a hydrogen molecule in an intense, near-infrared laser field. Numerical results are presented to demonstrate that the time-dependent numerical multiconfiguration wave function is able to describe the correlated electron motions as well as the ionization processes of a molecule in intense laser fields. © *2008 American Institute of Physics*. [DOI: 10.1063/1.2912066]

I. INTRODUCTION

Recent progress of high power laser technology has opened up a new field of atomic and molecular science. Novel phenomena induced by ultrafast electronic dynamics of atoms and molecules interacting with intense, ultrashort near-infrared (IR) laser pulses, such as tunnel ionization[1] and high-harmonic generation (HHG) of emission,[2] have been discovered. It is well known that x-ray pulses of hundred attosecond duration can be generated by precise control of HHG of atoms.[3] Time resolution of measurements of physical or chemical processes has now reached down to the attosecond regime. This means that we have already acquired a new tool to reveal the ultrafast dynamics of electrons in atoms and molecules and the initial processes of photochemical reactions.[4–6]

The high power laser is also a tool to induce various types of chemical reactions. Bond selectivity can be enhanced by simply changing the intensity or pulse duration. In fact, a more sophisticated way of controlling reaction dynamics by intense laser pulses has already been widely used. For example, Assion *et al.*[7] used intense near-IR femtosecond laser pulses tailored by a genetic algorithm-controlled pulse shaper to optimize the branching ratios of different organometallic photodissociation channels.

Analysis and investigation of these ultrafast phenomena including chemical reactions require accurate theoretical descriptions of electronic dynamics in the nonperturbative regime of light-matter interaction. It is thus desired to numerically solve the corresponding time-dependent Schrödinger equation (TDSE) as accurately as possible. Numerically rigorous solution of the TDSE is, however, limited to few-electron systems at present.[8–11] Electron correlation is only partially taken into account in the time-dependent density functional method used for the investigation of many-electron dynamics. On the other hand, the quantum chemical approach based on molecular orbital theory can provide an adequate description of the electronic structures of many-electron systems. The tractability of the quantum chemical approach in the treatment of many-electron systems has already accelerated attempts to develop new time-dependent molecular orbital theories. As one of the attempts, time-dependent multiconfiguration (TDMC) theories have been developed.[12,13] The TDMC theory proposed in Ref. 12 is intended to describe the electronic (ionization) dynamics of one-dimensional (1D) model molecules in intense laser fields. In a previous study,[13] we formulated a TDMC self-consistent field (TDMCSCF) theory for real three dimensional (3D) molecules to derive the equations of motion (EOMs) for time-dependent molecular orbitals and configuration interaction coefficients. We employed Gaussian-type atomic orbital functions as a basis set to reproduce intramolecular charge transfer in a hydrogen molecule interacting with an intense near-IR pulse. Although there also exist many relevant investigations on the theoretical formulation[14–17] with applications to electronic dynamics of few-electron systems,[18–20] EOMs for 3D systems that describe continuum state dynamics as well as intramolecular bound-state dynamics have not yet been completely established.[21]

In this paper, we first formulate general EOMs for numerical orbital functions in coordinate representation on the basis of the TDMCSCF theory developed in our previous study for 3D molecules.[13] The EOMs of this numerical multiconfiguration time-dependent Hartree-Fock (MCTDHF) theory are then adapted to those suitable for the studies of diatomic (or linear) molecules. Illustrative numerical results for a hydrogen molecule in an intense laser field are presented to demonstrate that the numerical multiconfiguration

[a)]Author to whom correspondence should be addressed. Electronic mail: tkato@chem.s.u-tokyo.ac.jp.
[b)]Electronic mail: hirohiko-kono@mail.tains.tohoku.ac.jp.

wave function is able to describe the correlated electron motions as well as the ionization processes of molecules in intense laser fields.

II. THEORY

In this section, we first derive a general expression of the EOMs for the spin orbitals within the prescription of the time-dependent multiconfiguration theory in the coordinate representation, i.e., MCTDHF equation. Then, we tailor the EOMs to apply the theory to the electronic dynamics of diatomic (or linear) molecules.

Here, we briefly review the basic equations [Eqs. (6)–(10)] that have been derived in Ref. 13 and develop the time-dependent multiconfiguration theory in the coordinate representation. The EOM for the orbital function [Eq. (6)] can be integrated for both the Gaussian-type atomic orbital functions and the numerical orbital functions. By utilizing the numerical orbital functions, we are able to describe large amplitude motion of electrons in a molecule that are hardly represented by the use of localized basis functions such as Gaussian-type atomic orbital functions.

The electronic Hamiltonian in the Born–Oppenheimer approximation is given by

$$\hat{H} = \sum_{ij} h_{ij}(t)\hat{a}_i^\dagger \hat{a}_j + \frac{1}{2}\sum_{ijkl}[ki|lj]\hat{a}_k^\dagger \hat{a}_l^\dagger \hat{a}_j \hat{a}_i, \tag{1}$$

where $\hat{a}_i$ and $\hat{a}_i^\dagger$ denote the annihilation and creation operators for an electron in the ith spin orbital, respectively. The time-dependent single-particle integral $h_{ij}(t)$ contains three terms: the kinetic energy operator for the electron, the attraction potential between the electron and the nuclei, which is denoted by $\hat{V}_{\mathrm{nucl}}(\vec{r})$, and the time-dependent external potential $\hat{V}_{\mathrm{ext}}(t)$. The explicit form of $h_{ij}(t)$ is given by

$$h_{ij}(t) = \int d\vec{x}\psi_i^*(\vec{x})\left\{-\frac{\hbar^2}{2m_e}\nabla^2 + V_{\mathrm{nucl}}(\vec{r}) + V_{\mathrm{ext}}(t)\right\}\psi_j(\vec{x}), \tag{2}$$

where m_e is the electron mass and $\vec{x}=(\vec{r},\sigma)$ denotes the spatial and the spin coordinates of an electron. $\psi_i(\vec{x})=\langle \vec{x}|i\rangle$ is the ith spin-orbital function. The two-particle integral $[ki|lj]$ represents the Coulomb interactions between electrons, and is given by

$$[ki|lj] = \frac{1}{4\pi\epsilon_0}\int d\vec{x}_1 d\vec{x}_2 \psi_k^*(\vec{x}_1)\psi_i(\vec{x}_1)\frac{e^2}{|\vec{r}_1-\vec{r}_2|}\psi_l^*(\vec{x}_2)\psi_j(\vec{x}_2), \tag{3}$$

where e is the charge of an electron and ϵ_0 is the permittivity of vacuum.

A normalized multiconfiguration N-electron wave function serves as the starting point of the theory. It is given by a linear combination of Slater determinants as[12,13]

$$\Phi = \sum_{I=1}^{M} C_I \Phi_I, \tag{4}$$

where C_I is a complex coefficient (called CI-coefficient), M is a possible number of the Slater determinants for a given set of molecular orbitals. An N-electron Slater determinant Φ_I is explicitly represented by specifying constituent spin-orbitals ψ_i as

$$\Phi_I = \|\psi_{i_1}\psi_{i_2}\cdots\psi_{i_N}\| \quad (i_1 < i_2 < \cdots < i_N). \tag{5}$$

We refer to the spin orbitals used in the CI expansion of Eq. (4) as *occupied* spin orbitals. The number of occupied spin orbitals will be denoted by N_o. Note that the spin-orbital functions as well as the CI coefficients depend on time t in the present theory. The variable t involved in these quantities are omitted in Eqs. (1)–(5) for the sake of simplicity.

A. The EOM for the spin-orbital functions in the coordinate representation

The basic EOM for the occupied spin orbitals is given in Ref. 13 as

$$i\hbar\frac{\partial}{\partial t}\vec{X}(r) = \boldsymbol{A}^{-1}(t)[\hat{\boldsymbol{K}}(t) - \boldsymbol{\Lambda}(t)]\vec{X}(t), \tag{6}$$

where $(\vec{X}(t))_m = \psi_m(t) = |m(t)\rangle (1 \leqslant m \leqslant N_o)$. In Eq. (6), we write the $(N_o \times N_o)$ first order reduced density matrix $\mathbf{A}$ as

$$A_{km}(t) = \sum_{I}^{(k)} (-1)^{p_I(k)+p_J(m)} C_I^*(t) C_{kI}^m(t), \tag{7}$$

where $C_{kI}^m(t)$ denotes the CI coefficient for a determinant that is constructed from the determinant Φ_I by a single substitution $\psi_m \leftarrow \psi_k$ and the symbol $p_I(k)$ stands for the *position* of the kth spin orbital in Φ_I, e.g., $p_I(k)=j$ if $i_j=k$ in Eq. (5). We refer to the determinant that is made from these substitution(s) in Φ_I, i.e., Φ_{kI}^m, as just Φ_J as long as there is no confusion; e.g., J of $p_J(m)$ in Eq. (7) stands for Φ_{kI}^m.

The $(N_o \times N_o)$ matrix operator $\hat{\mathbf{K}}$ is given by

$$\hat{K}_{km}(t) = A_{km}(t)\hat{h}(t) + \hat{V}_{km}(t), \tag{8}$$

where $\hat{h}(t)$ is the single-particle operator corresponding to the first term of the Hamiltonian of Eq. (1) and the elements of the potential operator $\hat{\boldsymbol{V}}(t)$ are given by

$$\hat{V}_{km}(t) = \sum_{I}^{(k)} (-1)^{p_I(k)+p_J(m)} C_I^*(t) \left[C_{kI}^m(t)\{\hat{V}^{(I)}(t) - (\hat{J}_k(t) - \hat{K}_k(t))\} + \sum_{n}^{\text{occ}I} \sum_{I(\neq m)}^{\text{occ}} (-1)^{p_I(n)+p_J(l)} C_{knI}^{lm}(t) \text{sgn}(k-n)\text{sgn}(m-l) \hat{f}_{nl}(t) \right]. \tag{9}$$

Here, $C_{knI}^{lm}(t)$ denotes the CI coefficient for a determinant that is constructed from Φ_I by a double substitution $(\psi_l, \psi_m) \leftarrow (\psi_k, \psi_n)$. $\hat{V}^{(I)}(t)$ denotes a potential associated with a Slater determinant Φ_I and is given by $\hat{V}^{(I)}(t) = \Sigma_s^{\text{occ}I}(\hat{J}_s(t) - \hat{K}_s(t))$, where $\hat{J}_s$ and $\hat{K}_s$ are Coulomb and exchange operators, respectively, defined to give the matrix elements, $\langle i|\hat{J}_s(t)|j\rangle = [ij|s(t)s(t)]$, and $\langle i|\hat{K}_s(t)|j\rangle = [is(t)|s(t)j]$. The general two-particle operator $\hat{f}_{kl}$ in Eq. (9) is defined by $\langle i|\hat{f}_{kl}(t)|j\rangle = [ij|k(t)l(t)]$. The definition of the ranges of summation is given in Ref. 13. The Lagrange multiplier matrix $\mathbf{\Lambda}$ is introduced to keep the occupied spin orbitals to form an orthonormal basis set. Here, we employ the following form according to our previous study[13,15]

$$\Lambda_{nm}(t) = \sum_{k}^{\text{occ}} \langle m(t)|\hat{K}(t)_{nk}|k(t)\rangle \quad (1 \leqslant n,m \leqslant N_o). \tag{10}$$

This choice of the Lagrange multiplier matrix ensures that the time evolution of the occupied spin orbitals be unitary, i.e., $\langle k(t)|\partial/\partial t|m(t)\rangle = 0$ with the initial condition $\langle k(t_0)|m(t_0)\rangle = \delta_{km}$ $(1 \leqslant k,m \leqslant N_o)$ [see Eq. (18)].

Substitution of Eq. (8) into Eq. (6) yields

$$i\hbar \frac{\partial}{\partial t}\vec{X}(t) = [\hat{h}(t)1 + \boldsymbol{A}^{-1}(t)\{\hat{\boldsymbol{V}}(t) - \mathbf{\Lambda}(t)\}]\vec{X}(t). \tag{11}$$

Of particular importance for numerical integrations of Eq. (11) in coordinate representation is to rewrite the potential operator $\hat{\boldsymbol{V}}(t)$ in terms of local operators $\hat{f}_{kI}$ as

$$\hat{\boldsymbol{V}}(t) = \sum_{nl}^{\text{occ}} \hat{\boldsymbol{V}}^{(nl)}(t) \tag{12a}$$

with

$$\hat{V}_{ij}^{(nl)}(t) = v_{ij}^{(nl)}(t)\hat{f}_{nl}(t) \quad (1 \leqslant i,j \leqslant N_o). \tag{12b}$$

Equation (9) allows us to express the coefficient $v_{ij}^{(nl)}$ in terms of CI coefficients as

$$\begin{aligned} v_{ij}^{(nl)}(t) = \sum_{I}^{(i)} \{\theta(n,I) - \delta_{ni}\} C_I^*(t)[\delta_{nl}(-1)^{p_I(i)+p_J(j)} C_{iI}^j(t) \\ - \delta_{nj}(-1)^{p_I(i)+p_J(l)} C_{iI}^l(t)] \\ + \sum_{I}^{(i\neq n)} \text{sgn}(i-n)\text{sgn}(j-l)\bar{\delta}_{(i,n),(j,l)} \\ \times (-1)^{p_I(i)+p_I(n)+p_J(j)+p_J(l)} C_I^*(t) C_{inI}^{lj}(t), \end{aligned} \tag{13}$$

where $\theta(n,I)$ is nonzero (unity) only if the spin-orbital ψ_n is a constituent orbital of Φ_I, and $\bar{\delta}_{(i,n),(j,l)} = (1-\delta_{ij})(1-\delta_{nl})(1-\delta_{il})(1-\delta_{nj})$. Equation (11) now reads

$$i\hbar \frac{\partial}{\partial t}\vec{X}(t) = \left[\hat{h}(t)1 + \boldsymbol{A}^{-1}(t)\left\{ \sum_{nl}^{\text{occ}} \hat{\boldsymbol{V}}^{(nl)}(t) - \mathbf{\Lambda}(t) \right\} \right] \vec{X}(t). \tag{14}$$

The equivalence of Eqs. (14) and (11) is directly confirmed by substituting Eqs. (12a), (12b), and (13) into Eq. (14).

We notice that in Eq. (14) the nonlocal exchange potentials found in Eq. (9) are eliminated so that all the electron-electron interaction potentials are expressed as local potentials of $\hat{f}_{nl}$. The complex-valued coefficient $v_{ij}^{(nl)}$ governs the magnitude of the orbital coupling between the ith and the jth spin orbitals mediated by the presence of electrons occupying the nth and the lth spin orbitals. A similar expression of the two-particle operator in a local potential form has recently been formulated with the help of the second order reduced density matrix for systems composed of fermions and/or bosons.[22]

Equation (14) is further simplified as

$$i\hbar \frac{\partial}{\partial t}\vec{X}(t) = \left[\hat{h}(t)1 + \sum_{nl}^{\text{occ}} \tilde{\boldsymbol{v}}^{(nl)}(t)\hat{f}_{nl}(t) - \tilde{\mathbf{\Lambda}}(t) \right] \vec{X}(t), \tag{15}$$

where we denote $\tilde{\mathbf{v}}^{(nl)}(t) = \boldsymbol{A}^{-1}(t)\mathbf{v}^{(nl)}(t)$ and $\tilde{\mathbf{\Lambda}}(t) = \boldsymbol{A}^{-1}(t)\mathbf{\Lambda}(t)$. The explicit EOM for the kth $(1 \leqslant k \leqslant N_o)$ spin orbital is reduced from Eq. (15) as

$$i\hbar \frac{\partial}{\partial t}|k(t)\rangle = \hat{h}(t)|k(t)\rangle + \sum_{j}^{\text{occ}} \left[\sum_{nl}^{\text{occ}} \tilde{v}_{kj}^{(nl)}(t)\hat{f}_{nl}(t) - \tilde{\Lambda}_{kj}(t) \right] |j(t)\rangle. \tag{16}$$

By using Eqs. (8) and (10), we can determine the modified Lagrange multipliers as

$$\begin{aligned} \tilde{\Lambda}_{kj}(t) &= (\boldsymbol{A}^{-1}(t)\mathbf{\Lambda}(t))_{kj} \\ &= \langle j(t)|\hat{h}(t)|k(t)\rangle + \sum_{q}^{\text{occ}} \sum_{nl}^{\text{occ}} \tilde{v}_{kq}^{(nl)}(t)\langle j(t)|\hat{f}_{nl}(t)|q(t)\rangle, \end{aligned} \tag{17}$$

which ensures that the occupied orbitals propagate into the complementary space with respect to the current occupied spin orbitals:

$$i\hbar\frac{\partial}{\partial t}|k(t)\rangle = \hat{Q}(t)\left[\hat{h}(t)|k(t)\rangle + \sum_{nl}^{\text{occ}}\sum_{j}^{\text{occ}}\tilde{v}_{kj}^{(nl)}(t)\hat{f}_{nl}(t)|j(t)\rangle\right], \tag{18}$$

where $\hat{Q}(t)=\hat{1}-\Sigma_s^{\text{occ}}|s(t)\rangle\langle s(t)|$ is a time-dependent projector onto the orthogonal complement to the space spanned by the current occupied spin orbitals. Note that Eq. (18) can be integrated only with the information of occupied spin orbitals, in contrast to the case of TDMCSCF formalism where the EOM for the occupied spin orbitals is integrated by referencing unoccupied spin orbitals.[13]

B. EOMs for the spin-orbital functions with angular momentum restrictions

For the description of the electronic structure and the dynamics of a diatomic (or a linear) molecule, it is convenient to express the spatial orbital function χ as an eigenfunction of the orbital angular momentum component along the molecular axis ($\equiv\hat{l}_z$). For example, in the cylindrical coordinate system (ρ,z,ϕ), it takes the form of

$$\chi^{(m)}(\vec{r}) = e^{im\phi}\psi(\rho,z), \tag{19}$$

where the integer m stands for the eigen value for $\hat{l}_z/\hbar$. We will refer to the orbital function of the form of Eq. (19) as an *m-adapted* function. From Eq. (16), we can see that the m-adapted orbital functions are coupled with each other. Consequently, the time-evolving spin orbitals cannot, in general, be m-adapted. This is because the operator of $\hat{l}_z$ for each electron does not commute with the total Hamiltonian due to the presence of the electron-electron interactions. To keep the spin orbitals being m-adapted, we have to restrict the range of the orbital couplings in the general EOM of Eq. (15). To this end, we shall decompose the coefficient $\tilde{v}_{kj}^{(nl)}$ by multiplying it by a unit tensor $1\equiv\delta_{mm'}+\bar{\delta}_{mm'}$ as

$$\tilde{v}_{kj}^{(nl)}(t) = \delta_{m_k,m_j-m_n+m_l}\tilde{v}_{kj}^{(nl)}(t) + \bar{\delta}_{m_k,m_j-m_n+m_l}\tilde{v}_{kj}^{(nl)}(t) = \tilde{v}_{kj}^{(nl)'}(t) + \tilde{v}_{kj}^{(nl)''}(t), \tag{20}$$

where m_k denotes the angular momentum projection of the kth (m-adapted) spin orbital onto the molecular axis. In Eq. (20), we intend to separate the orbital couplings into two types by using the change in the angular momentum projection of the kth spin orbital, Δm_k. We see that $\tilde{v}_{kj}^{(nl)'}$ corresponds to the couplings with $\Delta m_k=0$ and $\tilde{v}_{kj}^{(nl)''}$ with $\Delta m_k\neq 0$. These are simply deduced from the fact that the action of $\hat{f}_{nl}$ on $|j\rangle$ generates an angular momentum projection of $m=m_j-m_n+m_l$ provided that the orbitals are m-adapted, i.e., $\langle\vec{r}|\hat{f}_{nl}|\chi_j^{(m_j)}\rangle\propto\exp[i(m_j-m_n+m_l)\phi]$. Accordingly, the modified Lagrange multiplier of Eq. (17) is decomposed as

$$\tilde{\Lambda}_{kj}(t) = \langle j(t)|\hat{h}(t)|k(t)\rangle + \sum_{q}^{\text{occ}}\sum_{nl}^{\text{occ}}\tilde{v}_{kq}^{(nl)'}(t)\langle j(t)|\hat{f}_{nl}(t)|q(t)\rangle + \sum_{q}^{\text{occ}}\sum_{nl}^{\text{occ}}\tilde{v}_{kq}^{(nl)''}(t)\langle j(t)|\hat{f}_{nl}(t)|q(t)\rangle. \tag{21}$$

If we use the notations

$$\tilde{\Lambda}'_{kj}(t) = \delta_{m_k m_j}\langle j(t)|\hat{h}(t)|k(t)\rangle + \sum_{q}^{\text{occ}}\sum_{nl}^{\text{occ}}\tilde{v}_{kq}^{(nl)'}(t)\langle j(t)|\hat{f}_{nl}(t)|q(t)\rangle \tag{22a}$$

and

$$\tilde{\Lambda}''_{kj}(t) = \bar{\delta}_{m_k m_j}\langle j(t)|\hat{h}(t)|k(t)\rangle + \sum_{q}^{\text{occ}}\sum_{nl}^{\text{occ}}\tilde{v}_{kq}^{(nl)''}(t)\langle j(t)|\hat{f}_{nl}(t)|q(t)\rangle, \tag{22b}$$

substitution of Eqs. (20), (22a), and (22b) into Eq. (16) yields another expression of the general EOM for the occupied orbitals as

$$i\hbar\frac{\partial}{\partial t}|k(t)\rangle = \hat{P}^{(m_k)}\hat{h}(t)|k(t)\rangle + \sum_{j}^{\text{occ}}\left[\sum_{nl}^{\text{occ}}\tilde{v}_{kj}^{(nl)'}(t)\hat{f}_{nl}(t) - \tilde{\Lambda}'_{kj}(t)\right]|j(t)\rangle + \hat{Q}^{(m_k)}\hat{h}(t)|k(t)\rangle + \sum_{j}^{\text{occ}}\left[\sum_{nl}^{\text{occ}}\tilde{v}_{kj}^{(nl)''}(t)\hat{f}_{nl}(t) - \tilde{\Lambda}''_{kj}(t)\right]|j(t)\rangle, \tag{23}$$

in which the couplings of the occupied spin orbitals are divided into the couplings conserving the angular momentum projection ($\Delta m_k=0$, the second term) and the nonconserving one ($\Delta m_k\neq 0$, the fourth term). The action of the single-particle part $\hat{h}(t)$ is also separated; $\hat{P}^{(m_k)}$ denotes the projector onto the eigen space associated with the quantum number m_k of $\hat{l}_z/\hbar$ (the first term), and $\hat{Q}^{(m_k)}$ is defined as $\hat{1}-\hat{P}^{(m_k)}$ (the third term).

By ignoring the last two terms in Eq. (23) on purpose, we arrive at an EOM

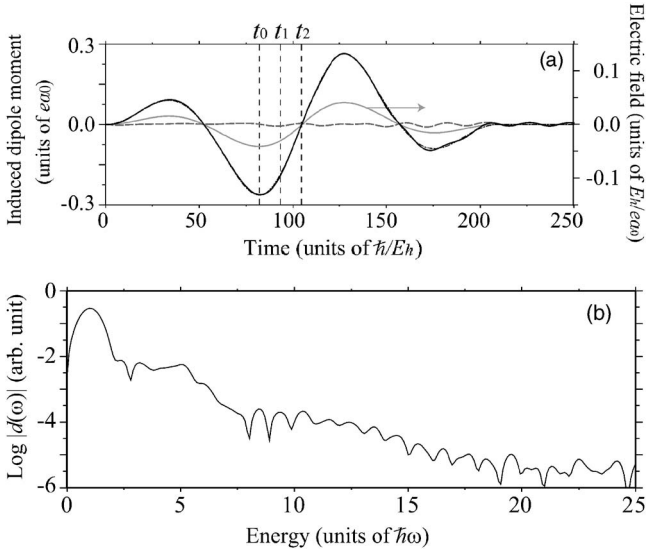

FIG. 1. (a) The time dependence of the induced dipole moment of H_2 in an intense, near-IR laser field (solid line). The gray line shows the amplitude of the laser electric field (wavelength: $\lambda=760$ nm, intensity for the maximum field strength: $I=5.8\times10^{13}$ W/cm^2). The dotted-broken line shows an adiabatic fit of the induced dipole moment in termes of the polarizabilites up to the second order hyper polarizability. The gray broken line shows the difference of the former from the latter. (b) The power spectrum of the induced dipole moment as a function of emitted photon energy. We use time points t_0, t_1, and t_2 in the following discussion.

$$i\hbar\frac{\partial}{\partial t}|k(t)\rangle = \hat{P}^{(m_k)}\hat{h}(t)|k(t)\rangle + \sum_j^{\text{occ}}\left[\sum_{nl}^{\text{occ}}\tilde{v}_{kj}^{(nl)\prime}(t)\hat{f}_{nl}(t) - \tilde{\Lambda}'_{kj}(t)\right]|j(t)\rangle = \hat{Q}(t)\left[\hat{P}^{(m_k)}\hat{h}(t)|k(t)\rangle + \sum_j^{\text{occ}}\sum_{nl}^{\text{occ}}\tilde{v}_{kj}^{(nl)\prime}(t)\hat{f}_{nl}(t)|j(t)\rangle\right], \tag{24}$$

which conserves the angular momentum projection of m-adapted orbital functions. Equation (24) is regarded as our working equation for calculating the electronic dynamics of diatomic (or linear) molecules. In a context of the variation principle, the above restriction of the range of the functional space is considered to degrade the flexibility of the wave function. However, it can be compensated by including m-adapted spin orbitals of large $|m|$ into the set of occupied spin orbitals. Furthermore, Eq. (24) allows us to propagate the orbital functions in two-dimensional space, i.e., ρ and z. Manipulation of the function of ϕ can be treated analytically. This reduction in the dimensionality greatly reduces the computation cost in comparison with three-dimensional implementations.

III. APPLICATION TO THE HYDROGEN MOLECULE

In the following, we apply the present method to simulate the electronic dynamics of a hydrogen molecule in an intense near-infrared laser field. We use Eq. (24) as the EOM for the spin-orbitals. The dual transformation technique developed by Kono and co-workers[23,24] is used to properly take into account the operation of the electron-nucleus Coulomb potentials and the kinetic energy operators on the numerical orbital functions. For the action of the operators $\hat{f}_{nl}$ in Eq. (24) we utilize a Legendre expansion of r^{-1} to construct time-independent electron-electron interaction kernels[25] that depend on the absolute value of the difference in the angular momentum projection, $|-m_n+m_l|$.

To obtain the singlet ground state wave function by imaginary time propagation, we used nine spatial MOs, $(1\sigma_g)$, $(1\sigma_u, 1\pi_u^{\pm}, 2\sigma_g)$, and $(1\pi_g^{\pm}, 3\sigma_g, 2\sigma_u)$, of which the HF orbital energies are roughly grouped into three. The total number of Slater determinants used to expand the wave function of Eq. (4) is 81. The grid points to describe the numerical orbital functions are set in the rectangular space of $|z| \leqslant 39.8a_0$ and $\rho \leqslant 20.0a_0$, where a_0 is the Bohr radius. The numbers of the grid points for z and ρ are 200 and 50, respectively. The electronic ground state energy is calculated to be $E_g=-1.7820E_h$ for the internuclear distance of $R=1.6a_0$, where E_h is the Hartree energy. The exact value is $E_{\text{exact}}=-1.7936E_h$.[26]

Now, we consider a hydrogen molecule interacting with an intense laser field. We adopt the dipole approximation in the length gauge for the laser-molecule interaction. The electric field is assumed to have a form $\vec{\mathcal{E}}(t)=\vec{e}_z f(t)\sin(\omega t)$, where the polarization vector $\vec{e}_z$ is parallel to the molecular axis. The envelope function $f(t)$ is linearly ramped so that $f(t)$ attains its maximum value of $f_{\max}$ at the first optical period of $t=T_c=2\pi/\omega$ and linearly damped within the next optical period. The laser frequency of this two-cycle pulse is $\omega=0.06E_h/\hbar$ (wavelength $\lambda=760$ nm, $T_c=104.7\hbar/E_h=2.53$ fs), and the field amplitude is set to be $f_{\max}=0.0534E_h/ea_0$ (the light intensity for the maximum field strength $\mathcal{E}_{\max}=0.0408E_h/ea_0$ is $I=5.8\times10^{13}$ W/cm^2). The evolution of the wave function of Eq. (4) is traced by simultaneously integrating the EOMs for the spin orbitals and the

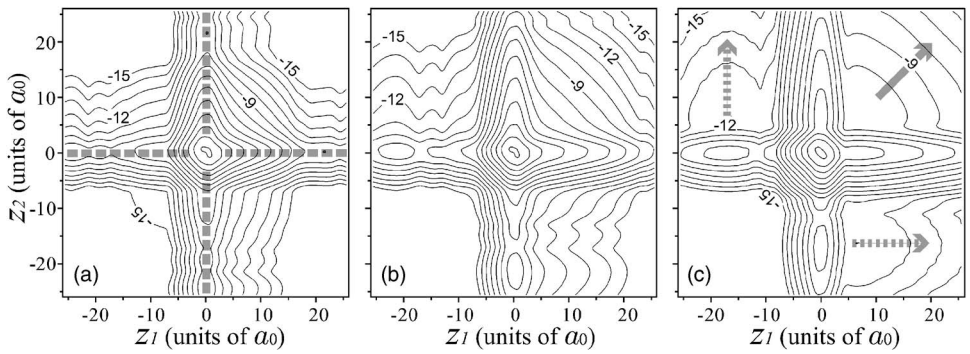

FIG. 2. Contour plot of the reduced density function $P(z_1,z_2,t)$ of H_2: Three snapshots in (a), (b), and (c) are those at three time points $t_0=82.00\hbar/E_h$, $t_1=93.36\hbar/E_h$, and $t_2=104.72\hbar/E_h$ indicated in Fig. 1(a), respectively. A logarithmic scale is employed. The wavelength of the two-cycle laser pulse is $\lambda=760$ nm and the intensity for the maximum field strength is $I=2.1\times10^{14}$ W/cm^2.

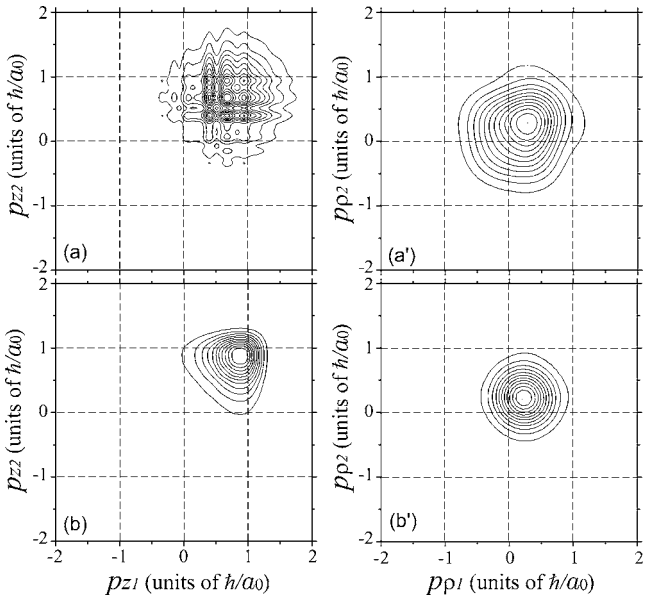

FIG. 3. Left: contour plot of the reduced density function $P(p_{z1},p_{z2},t)$. Right: the contour plot of the difference of the conditional reduced density function $\Delta P(p_{\rho 1},p_{\rho 2},t)$. (a) and (a′), and (b) and (b′) correspond to the time points t_0 and t_2 shown in Fig. 1(a), respectively. The laser parameters are the same as used in Fig. 2.

EOM for the CI-coefficients which is given, for example, in Refs. 13, 15, and 27. The time step is set to be $\Delta t = 0.005\hbar/E_h$ ($\hbar/E_h = 0.0242$ fs). We remove the outgoing wave components at the grid boundaries by using a mask function. A self-consistent time integration, which takes into account the redundancy due to the use of the two kinds of variational parameters (namely, CI coefficients and orbital functions), is implemented to keep the norms of the orbital functions being unity during the propagation.

First, we calculated the induced dipole moment and its power spectrum to see the applicability of the present method to the strong field phenomena. The power spectrum of the induced dipole moment corresponds to the spectrum of HHG from the molecule. As shown in Fig. 1(a), the induced dipole moment adiabatically follows the applied electric field and it can be well reproduced in terms of polarizabilities up to the second order hyper polarizability, $\alpha = 5.74(ea_0)^2/E_h$, $\beta = 0.0(ea_0)^3/(E_h)^2$ and $\gamma = 4.18\times 10^2(ea_0)^4/(E_h)^3$. After $t \simeq 150\hbar/E_h$, the amplitude of the induced dipole moment deviates from the adiabatic behavior owing to the effects of nonadiabatic electronic dynamics and ionization.

In Fig. 1(b), we plot the power spectrum of the induced dipole moment as a function of energy, which is calculated by applying the so-called Parzen window function to the calculated induced dipole moment. The envelope of the spectrum ranges beyond $13\hbar\omega$. According to the analysis based on the three-step model,[28] the kinetic energy of the returning electron is characterized by two maximal values $E_1 = 0.41E_h$ and $E_2 = 0.32E_h$, where the tunneling time t_t and return time t_r are $(t_t,t_r) \sim (16\hbar/E_h, 102\hbar/E_h)$ and $(85\hbar/E_h, 150\hbar/E_h)$, respectively. The ionization potential of the hydrogen molecule is $I_p = 0.564E_h$, thus the two maximal kinetic energies correspond to the harmonic radiation of the order of 16 and 15, respectively. These energy values agree well with the existence of the cutoff energy around $15\hbar\omega$ in the power spectrum. From this agreement we conclude that the tunnelling and the subsequent recollision of the electron with the parent ion core can be described by the present method. This is reasonable because the ponderomotive radius $\alpha_p = e\mathcal{E}/m_e\omega^2$ is $\sim 11.3a_0$, which is about four times smaller than the grid size for the z direction.

We next present the results of wave packet dynamics in the case of $f_{\max} = 0.100E_h/ea_0$. (The maximum field strength $\mathcal{E}_{\max} = 0.0766E_h/ea_0$ corresponds to $I = 2.1\times 10^{14}$ W/cm^2.) The other parameters are the same as in Fig. 1. We introduce the reduced density function $P(z_1,z_2,t) = \Sigma_{\sigma_1,\sigma_2}\int dx_1dx_2dy_1dy_2|\Phi(\vec{x}_1,\vec{x}_2,t)|^2$ to visualize the two electron motion along the polarization direction of the electric field. We show in Fig. 2 three snapshots of $P(z_1,z_2,t)$ at $t_n = t_{\min} + n\tau$ ($n = 0$, 1, and 2), where $t_{\min} = 82.00\hbar/E_h$ is the time at the first minimum of the field and $\tau = (T_c - t_{\min})/2$. Three time points t_0, t_1, and t_2 are indicated in Fig. 1(a). The peak around $z_1 = z_2 = 0$ in Fig. 2 is the bound state component. The broad lobes of the electron density along the z_1 and z_2 axes in Fig. 2(a) indicate that ionization starts before time t_0 (broken lines). In the second half period of the laser electric

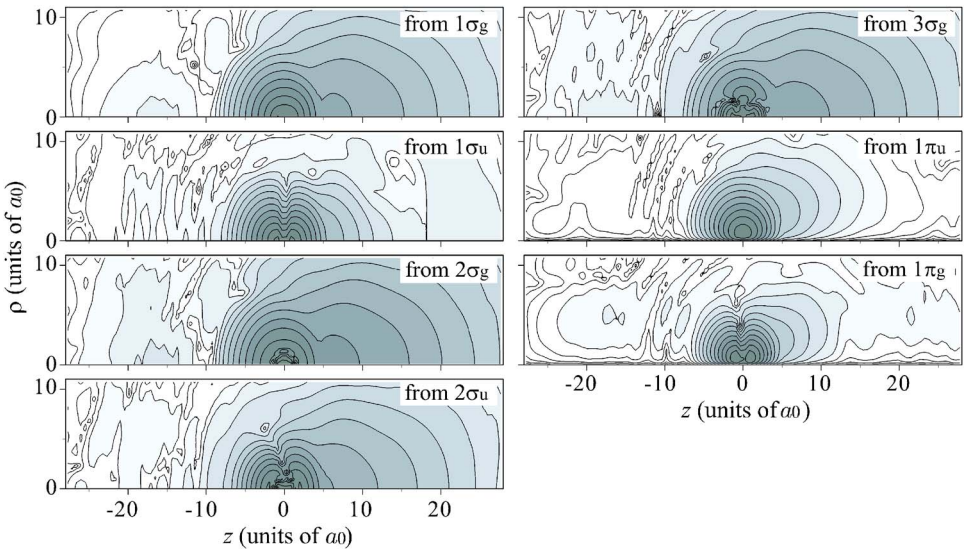

FIG. 4. (Color online) Contour plot of the modulus of the natural orbitals at time t_2 specified in Fig. 1(a). The symmetry symbols stand for the orbital symmetry when the molecule is in the electronic ground state, i.e., the initial state. A logarithmic grayscale is employed. The laser parameters are the same as used in Fig. 2.

field, it exerts on the electrons a force directed toward larger z. In addition to single-electron ionization, this force induces two types of double ionization: One is the stepwise emission of the two electrons in the opposite sides [for instance, the ionizing currents in the region of $z_1>0$ and $z_2<0$ indicated by a dotted arrow in Fig. 2(c)] and the other is the simultaneous emission of the electrons into the same side [solid arrow in Fig. 2(c)].[29,30] We can see from Fig. 2 that as time elapses from t_0 to t_2 the amplitude of the simultaneous emission increases as well as that of the step wise one. At early times the ionizing currents for both pathways have similar amplitudes as shown in Fig. 2(a), but at later times the amplitude of the simultaneous emission dominates the double ionization process [Fig. 2(c)]. This simultaneous electron emission is explained by the rescattering mechanism based on the three-step model: The kinetic energy of the returning electron at time $t\sim t_2$ takes a maximum value of $\sim 1.44E_h$ which is larger than the ionization potential of H_2^+ ($1.22E_h$ at the internuclear distance of $1.6a_0$). Thus, by the rescattering of the returning electron, the two electron can be emitted by sharing the recollision energy and the momentum as analyzed in the next paragraph. On the other hand, it has been reported that the second ionization in the stepwise electron emission process arises from the excited state of H_2^+.[30] For more detailed clarification of the mechanisms of these double ionization processes, it is further required to develop a technique to quantify and visualize the electron correlations in space and time.

We plot in Fig. 3 two kinds of reduced density functions in momentum space to reveal the detailed behavior of the two electrons in the simultaneous emission process. One is the distribution function of the momenta p_{z1} and p_{z2} of two electrons 1 and 2 along the z axis, $P(p_{z1},p_{z2},t)$, and the other is the difference between two conditional reduced density functions for $\phi_1=\phi_2+\pi$ and $\phi_1=\phi_2$: $\Delta P(p_{\rho 1},p_{\rho 2},t) = P(p_{\rho 1},p_{\rho 2},t)|_{\phi_1=\phi_2+\pi} - P(p_{\rho 1},p_{\rho 2},t)|_{\phi_1=\phi_2}$, where the total wave function is simply expanded in terms of plane waves $\exp[i(p_{\rho_1}\rho_1+p_{\rho_2}\rho_2)/\hbar]$.[31] The function $\Delta P(p_{\rho 1},p_{\rho 2},t)$ is introduced to examine the angular correlation of the two electrons. To obtain these density functions, we take into account the amplitude of the wave function for z_1, $z_2>9a_0$. Around $t=t_0$ the correlation with respect to p_z is not so high, but at later time t_2, the two electrons have nearly the same momentum along the z direction. The function $\Delta P(p_{\rho 1},p_{\rho 2},t)$ has a peak at $p_{\rho 1}=p_{\rho 2}>0$, which indicates that the two electrons avoid each other in the ϕ coordinate space and move toward larger ρ, i.e., the escape of the two electrons in the opposite direction. Notice that such the angular correlation cannot be obtained without the inclusion of orbital functions of $|m|>0$.

Finally, we plot in Fig. 4 the modulus of the natural orbitals at $t=t_2$. We can clearly see that the electron density spreads into large ρ region in spite of the interaction with the z-polarized electric field. The degree of the lateral spread seems larger in the σ orbitals than that in the π orbitals. Probably, this is due to the existence of the additional centrifugal potential $m^2/2\rho^2$ for non-σ orbitals.

IV. CONCLUDING REMARKS

We developed a time-dependent multiconfiguration theory for the simulation of electronic dynamics of molecules in intense laser fields and derived the equations of motion (EOMs) for spin orbitals in the coordinate representation. We derived Eq. (18) as the EOM for general nonlinear molecules and Eq. (24) as the EOM for linear molecules.

As an example of applications to linear molecules, we numerically solved Eq. (24) together with the EOM for the CI coefficients for a hydrogen molecule interacting with a near-infrared intense laser filed. The dual transformation for the linear molecule is employed for the grid representations of the spin orbitals. The obtained results for the hydrogen molecule have demonstrated that the single and double ionization processes of the molecule can be described by the present method. The angular electron correlation in the ionization process can be captured by including π orbitals, although the couplings between the orbitals represented by the last two terms in Eq. (23) are neglected in the working equation, i.e., Eq. (24).

Our results clearly showed that in the simultaneous double ionization process, the two electrons are ejected almost in the same direction parallel to the laser polarization direction (molecular axis), in agreement with the experimental results.[32] We conclude that the present approach is able to properly describe the angular electron correlation if we take into account an adequate number of spin orbitals of high $|m|$-values.

We would like finally to emphasize that the EOM of Eq. (18) have versatile applications to the dynamical processes of electrons such as Auger processes and electron-molecule collisions.

ACKNOWLEDGMENTS

The authors are grateful to Professor Y. Fujimura, Professor Y. Ohtsuki, Professor A. Fujii, and Professor K. Yamanouchi for their valuable discussions and encouragements. This research was partially supported by the Ministry of Education, Science, Sports and Culture, Grant-in-Aid for Scientific Research No. 1935001, Scientific Research on Priority Areas, "Control of Molecules in Intense Laser Fields" (No. 419), "Molecular Theory for Real Systems" (No. 461), Young Scientists (B) No. 17750003, and the Global COE Program for Chemistry Innovation.

[1] S. L. Chin, F. Yergeau, and P. Lavigne, J. Phys. B **18**, L213 (1985).
[2] X. F. Li, A. L'Huillier, M. Ferray, L. A. Lompre, and G. Mainfray, Phys. Rev. A **39**, 5751 (1989).
[3] M. Hentschel, R. Kienberger, Ch. Spielmann, G. A. Reider, N. Milosevic, T. Brabec, P. Corkum, U. Heinzmann, M. Drescher, and F. Krausz, Nature (London) **414**, 509 (2001).
[4] M. Drescher, M. Hentschel, R. Kienberger, M. Ulberracker, V. Yakovlev, A. Scrinzi, Th. Westerwalbesloh, U. Kleineberg, U. Heinzmann, and F. Krausz, Nature (London) **419**, 803 (2002).
[5] P. H. Bucksbaum, Science **317**, 766 (2007).
[6] K. Yamanouchi, Science **295**, 1659 (2002).
[7] A. Assion, T. Baumert, M. Bergt, T. Brixner, B. Kiefer, V. Seyfried, M. Strehle, and G. Gerber, Science **282**, 919 (1998).
[8] K. Taylor, Philos. Trans. R. Soc. London, Ser. A **360**, 1135 (2002).
[9] J. S. Parker, B. J. S. Doherty, K. T. Taylor, K. D. Schultz, C. I. Blaga, and L. F. DiMauro, Phys. Rev. Lett. **96**, 133001 (2006).
[10] K. Harumiya, I. Kawata, H. Kono, and Y. Fujimura, J. Chem. Phys. **113**,

8953 (2000).
[11] S. X. Hu and L. A. Collins, Phys. Rev. Lett. **96**, 073004 (2006).
[12] J. Zanghellini, M. Kitzler, C. Fabian, T. Brabec, and A. Scrinzi, Laser Phys. **13**, 1064 (2003).
[13] T. Kato and H. Kono, Chem. Phys. Lett. **392**, 533 (2004).
[14] J. Zanghellini, M. Kitzler, T. Brabec, and A. Scrinzi, J. Phys. B **37**, 763 (2004).
[15] J. Caillat, J. Zanghellini, M. Kitzler, O. Koch, W. Kreuzer, and A. Scrinzi, Phys. Rev. A **71**, 012712 (2005).
[16] T. T. Nguyen-Dang, M. Peters, S.-M. Wang, E. Sinelnikov, and F. Dion, J. Chem. Phys. **127**, 174107 (2007).
[17] O. E. Alon, A. I. Strelsov, and L. S. Cederbaum, Phys. Rev. A **76**, 062501 (2007).
[18] M. Nest and T. Klamroth, Phys. Rev. A **72**, 012710 (2005).
[19] M. Kitzler, J. Zanghellini, Ch. Jungreuthmayer, M. Smits, A. Scrinzi, and T. Brabec, Phys. Rev. A **70**, 041401(r) (2004).
[20] F. Remacle, M. Nest, and R. D. Levine, Phys. Rev. Lett. **99**, 183902 (2007).
[21] G. Jordan, J. Caillat, C. Ede, and A. Scrinzi, J. Phys. B **39**, S341 (2006).
[22] O. E. Alon, A. I. Strelsov, and L. S. Cederbaum, J. Chem. Phys. **127**, 154103 (2007).
[23] H. Kono, A. Kita, Y. Ohtsuki, and Y. Fujimura, J. Comput. Phys. **130**, 148 (1997).
[24] I. Kawata and H. Kono, J. Chem. Phys. **111**, 9498 (1999).
[25] M. Nest, T. Klamroth, and P. Saalfrank, J. Chem. Phys. **122**, 124102 (2005).
[26] W. Kolos and L. Wolniewicz, J. Chem. Phys. **43**, 2429 (1965).
[27] For the time-integration of CI-coefficients, we used the EXPOKIT software. R. B. Sidje, ACM Trans. Math. Softw. **24**, 130 (1998).
[28] P. B. Corkum, Phys. Rev. Lett. **71**, 1994 (1993).
[29] M. Lein, T. Kreibich, E. K. U. Gross, and V. Engel, Phys. Rev. A **65**, 033403 (2002).
[30] S. Baier, C. Ruiz, L. Plaja, and A. Becker, Phys. Rev. A **74**, 033405 (2006).
[31] The operator $(\hbar/i)\partial/\partial\rho$ cannot be a hermite operator for the orbital function represented in the cylindrical coordinate system. The alternative operator $(\hbar/i\sqrt{\rho})\partial/\partial\rho\sqrt{\rho}$, becomes hermite when the orbital function ψ, satisfies $\lim_{\rho\to 0}\rho|\psi|^2=0$ but the eigen function of this operator $(1/\sqrt{\rho})\exp[ip\rho/\hbar]$ does not satisfy above condition. We temporarily used the representation based on the eigen function for $(\hbar/i)\partial/\partial\rho$.
[32] D. Zeidler, A. Staudte, A. B. Bardon, D. M. Villeneuve, R. Dorner, and P. B. Corkum, Phys. Rev. Lett. **95**, 203003 (2005).